Antarctic Infra-Red Telescope with a 40cm primary mirror (AIRT40), Development and Improvement

Hirofumi Okita[a], Takashi Ichikawa[a], Tomohiro Yoshikawa[b], Ramsey Guy Lundock[a] and Kentaro Kurita[a]

[a]Astronomical Institute, Tohoku University, Aramaki Aoba Sendai 980-8578, Japan
[b]Koyama Astronomical Observatory, Kyoto Sangyo University, Motoyama, Kamigamo, Kita-ku, Kyoto 603-8555, Japan

ABSTRACT

Dome Fuji, on the Antarctic plateau, is expected to be one of the best sites for infra-red astronomy. In Antarctica, the coldest, driest air on Earth provides the deepest detection limit. Furthermore, the weak atmospheric turbulence above the boundary layer allows for high spatial resolution. We plan to perform site-testing at Dome Fuji during the austral summer of 2010-2011. This will be the first observation to use an optical/infra-red telescope at Dome Fuji. This paper introduces the Antarctic Infra-Red Telescope with a 40cm primary mirror (AIRT40) which will be used in this campaign; it is an infra-red Cassegrain telescope with a fork equatorial mount. AIRT40 will be used for not only site testing (measurement of seeing and sky background) and daytime astronomical observation during this summer campaign, but also for remote scientific observations during the 2012-2014 winter-over campaign. For this purpose, AIRT40 has to work well even at -80 degree Celsius. Therefore, we accounted for the thermal contraction of the materials while designing it, and made it with special parts which were tested in a freezer. For easy operation, many handles for transportation and a polar alignment stage were installed. Moreover, we confirmed that this telescope has enough pointing, tracking, and optical accuracy for the summer campaign through the test observations at Sendai, Japan. Because of these preparations AIRT40 is suited for observations at Dome Fuji. In the 2010-2011 campaign AIRT40 will be used to measure the seeing, infra-red sky background, and to observe Venus.

Keywords: Antarctica, Dome Fuji, infra-red telescope

1. INTRODUCTION

Infrared observation is important for researching distant galaxies, extrasolar planets, and star forming regions. Distant galaxies are observed at infra-red wavelengths because "normal" starlight (from ultraviolet to visible wavelengths) is red-shifted into the infra-red by the expanding universe. Extrasolar planets are lower temperature than the main stars, so that we can take higher contrast images of them at infra-red wavelength than with visible images. In addition, infra-red extinction by interstellar dust is weaker than visible extinction, this allows study of dust regions such as those in which stars are forming. However, it is difficult to observe infra-red rays from the ground. The infra-red sky background level is about 10,000 times as bright as the optical one due to airglow emission. And the thermal emissions from the atmosphere above observers and from a telescope itself exists. Furthermore, strong absorption lines of water vapor also exist at infra-red wavelengths. Therefore, it is important for ground-base infra-red astronomy to observe at the best site. So that infra-red astronomers thought of the possibility of observations on the Antarctic plateau, which has the lowest temperature and is a high altitude site. Due to the lowest temperature in the world, thermal noise is much lower than any other sites. The dry atmosphere with little water vapor is more transparent in infra-red wavelengths. It is said that the Antarctic plateau is the most suitable site for infra-red observations.

Site testing has been performed on the Antarctic Plateau at Dome C,[1,4] and Dome A.[11,12] The Japanese Antarctic station, Dome Fuji, is also located on the Antarctic plateau. Because of the low temperature and high

Further author information: (Send correspondence to H.Okita or T. Ichikawa)
H. Okita: E-mail: h-okita@astr.tohoku.ac.jp
T. Ichikawa: E-mail: ichikawa@astr.tohoku.ac.jp

Ground-based and Airborne Telescopes III, edited by Larry M. Stepp, Roberto Gilmozzi, Helen J. Hall
Proc. of SPIE Vol. 7733, 77331U · © 2010 SPIE · CCC code: 0277-786X/10/$18 · doi: 10.1117/12.856576

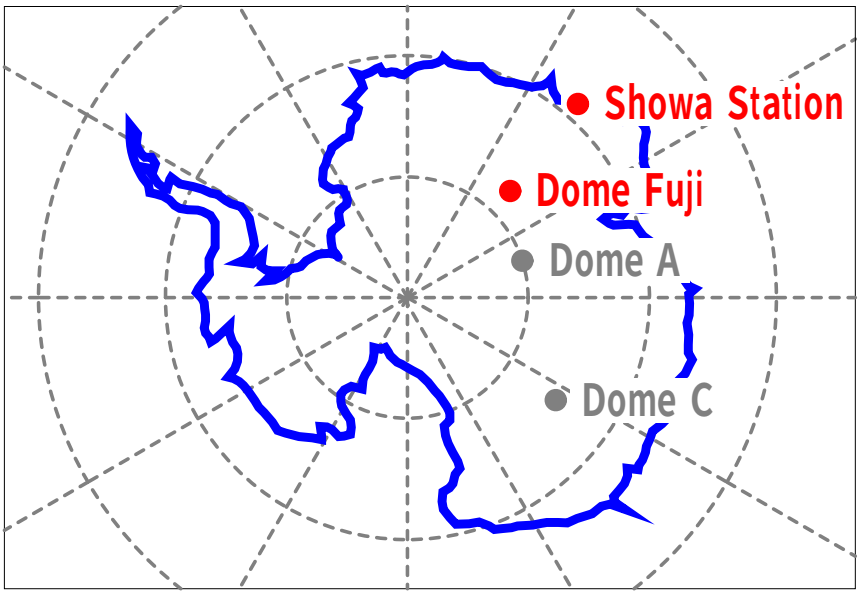

Figure 1. Location of Dome Fuji in Antarctica.

altitude, very little infra-red background is expected at Dome Fuji. Furthermore, the stable atmosphere at the domes on the Antarctic plateau leads good seeing.[8] To enjoy these advantages, we are planning to construct 2m-class infra-red telescopes at Dome Fuji. For this purpose we have performed site-testing at Dome Fuji since 2006. In this paper, we report the development and improvement of the Antarctic infra-red telescope, which will be used in the 2010-2011 summer campaign as the first optical/infra-red telescope at Dome Fuji.

2. DOME FUJI

Dome Fuji is one of the peaks of the Antarctic plateau and located at 77°19′01″S 39°42′12″E, which is 1,000km inland from Showa Station. Figure 1 shows the location of Dome Fuji. The altitude is 3,810m and it is the second highest next to Dome A (4,093m). The annual average temperature at the station is −54.4°C, and the lowest temperature ever recorded was −79.7°C.[10] It can be said that Dome Fuji is one of the coldest sites on Earth. This is a big advantage for infra-red observation. The Dome Fuji station was established by the National Institute of Polar Research of Japan (NIPR) in 1995. In the coming decade, NIPR plans to construct a permanent station at Dome Fuji for ice-core research and for "astronomy."

The 48th Japanese Antarctic Research Expedition (JARE) in 2006-2007 carried out site testing by using SODAR and a radiometer.[2,9] SODAR (SOnic Detection And Ranging) roughly measure the atmospheric turbulence up to the altitude of 1,000m. The radiometer measured the 220 GHz atmospheric-transparency, which is related to the total amount of water vapor in the atmosphere. The results of these experiments indicate a clear correlation between solar elevation and the turbulent layer height. The atmospheric-transparency in summer at Dome Fuji is comparable to at the Atacama Desert in Chile in their best seasons. In 2009-2010, the 51th JARE measured the absorption by the water vapor in the atmosphere by using a telescope-less infra-red spectrograph. The cloud cover was also observed by using an all-sky camera. These data are now being analyzed.

However, these observations were indirect measurement. The next (52th) JARE, plans to bring an optical/infra-red telescope to Dome Fuji to observe various site conditions (seeing, the height of the boundary layer, amount of water vapor, cloud cover, and infra-red sky background etc.) directly. This will be the first time to use an optical/infra-red telescope at Dome Fuji.

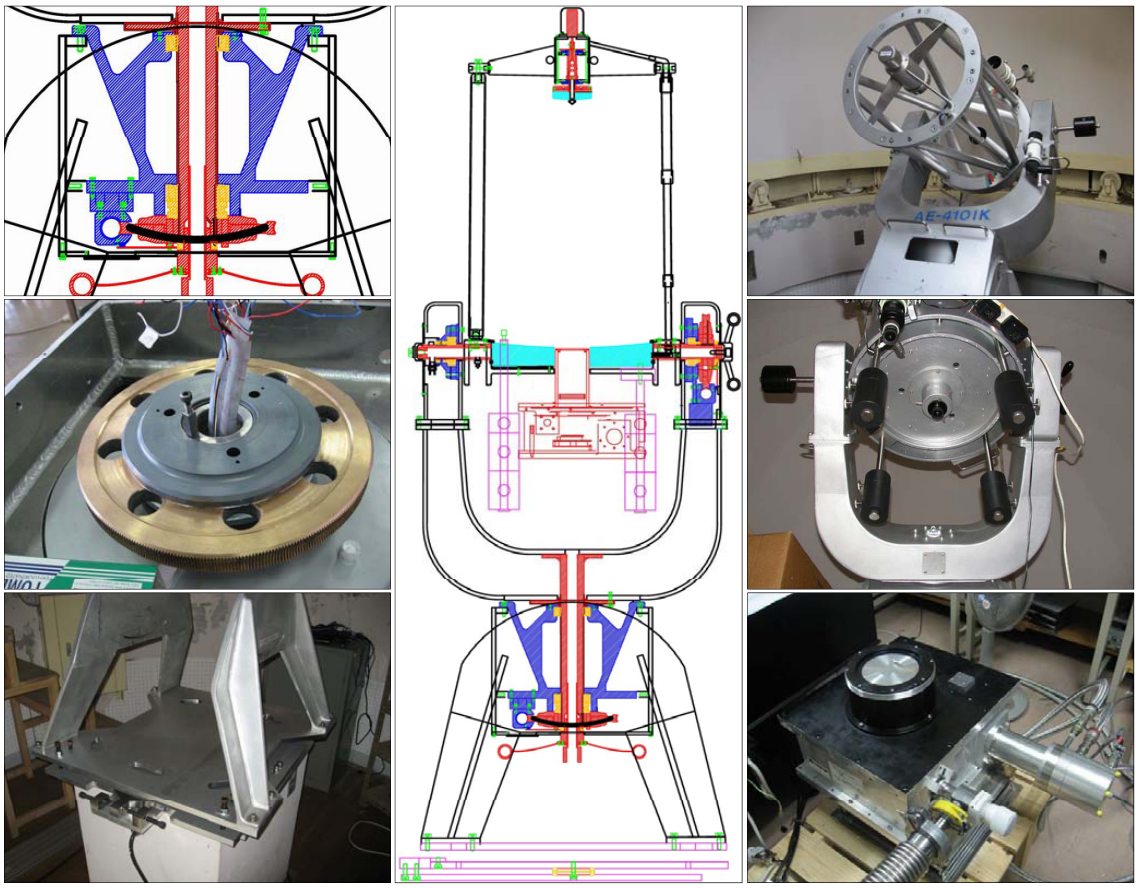

Figure 2. Left top: the cross-section of the RA Unit. Left middle: the clutch of Right Ascension axis. This clutch switches the rotation of the motor to a manual rotation. Left bottom: the polar alignment stage. The two axes can be moved independently. Center and rigth top: the design and a picture of AIRT40. Right middle: the balance adjuster. Right bottom: TONIC2 infra-red camera (Mode-B). It is under construction.

3. AIRT40

The Antarctic Infra-Red Telescope with a 40cm primary mirror (AIRT40) will be the first optical/infra-red telescope to be set up in Dome Fuji. AIRT40 was made to work well even at $-80°$C. It is a compact and light weight telescope for easy transportation. AIRT40 needs one computer for pointing, tracking, and focusing. Table 1 shows the specification of AIRT40. Some problems were found from the test observations in Sendai, Japan. We solved these problems with improvements to the original units and by developing additional parts. Figure 2 shows an outline and the details of AIRT40.

Table 1. Specification of AIRT40.

Parameter	**Specification**
Telescope type	Classic Cassegrain
Mount type	Equatorial
Diameter of the primary mirror	400mm
Diameter of the secondary mirror	100mm
Effective focal length	4,775mm
Total weight	$\sim$ 300kg
Operating temperature	$\geq -80°$C

3.1 RA Unit

The RA (Right Ascension) unit is composed of the shaft, the bearings, the holder, and the clutch of RA axis. The clutch of RA axis is a device which switches the rotation of the motor to a manual rotation. At first, because we had wanted to use grease as little as possible, we used a lamina of Teflon® as a clutch slider. Since the normal grease freezes at about $-50°C$, it is not possible to use it for AIRT40. However in the test observation, AIRT40 couldn't track a star correctly. It was thought that the cause was slip inside the RA clutch. So that we replaced the lamina of Teflon with Solvay Solexis FOMBLIN® ZLHT grease, which is soft even at $-80°C$. This new RA clutch had a cooling experiment with the freezer (see Section 4), and moved well at low temperatures. No slipping was observed after this improvement.

3.2 Polar Setting

AIRT40 is an equatorial telescope, so that it is necessary to set the RA axis to the south celestial pole correctly. For this adjustment, we developed the polar telescope and the polar alignment stage. The polar telescope is attached in parallel to the RA axis and it is used for polar alignment. The polar alignment stage has an altitude axis and an azimuth axis which can be moved independently. With these devices, we are able to set up AIRT40 accurately in only a few hours.

3.3 Balance Adjuster

AIRT40's loading capacity is about 40kg. However, if the balance of the telescope is not matched, it can't work accurately. Therefore, we installed the balance adjuster (counter weights) in AIRT40. This balance adjuster enables easy operation with various observational instruments installed on AIRT40.

3.4 Handles

We attached many handles for easy transportation and handling. It is very hard work to transport and build the telescope under cold environment and low atmospheric pressure at Dome Fuji.

3.5 TONIC2

TONIC2 (The TOhoku university Near Infra-red Camera II) is a near infra-red camera for AIRT40 using Reytheon VIRGO-2k astronomical array. TONIC2 is under construction in Tohoku University now. Two optical modes can be selected for TONIC2; Mode-A: narrow field of view (ϕ5 arcminute) camera with cold Lyot stop, and Mode-B: ϕ30 arcminute wide field of view direct camera. Because the cold Lyot stop cuts the light from the sky, Mode-A can observe with high signal to noise ratio (S/N). Figure 3 shows the optical lyout of Mode-A TONIC2. The lines represent the optical paths. We use the same CaF_2 singlet lens for collimator and camera. This simple optical system brings more higher efficiency, although there is only ϕ5 arcminute filed of view because of the coma aberration and field curvature. Mode-B TONIC2 is a direct camera which has no cold Lyot stop and has wide field of view. It is possible to observe with a high enough S/N without the cold Lyot stop since there is low thermal emission in the Antarctic winter.

We have planned observations that use Mode-A TONIC2 with J, H, K-band, and a few narrow-band filters during the austral summer of 2010-2011.

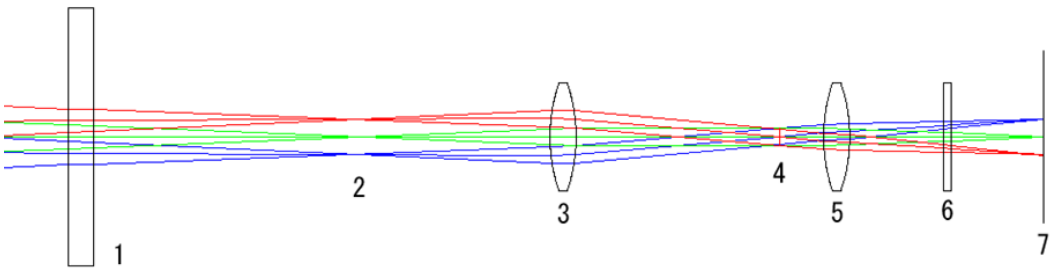

Figure 3. Optical layout of Mode-A TONIC2. The lines represent the optical paths. The numbered components are: 1) cryostat window; 2) focal plane of AIRT40; 3) collimator lens; 4) cold Lyot stop; 5) camera lens; 6) filter; 7) VIRGO-2k detector. The field of view of Mode-A TONIC2 is ϕ5 arcminute.

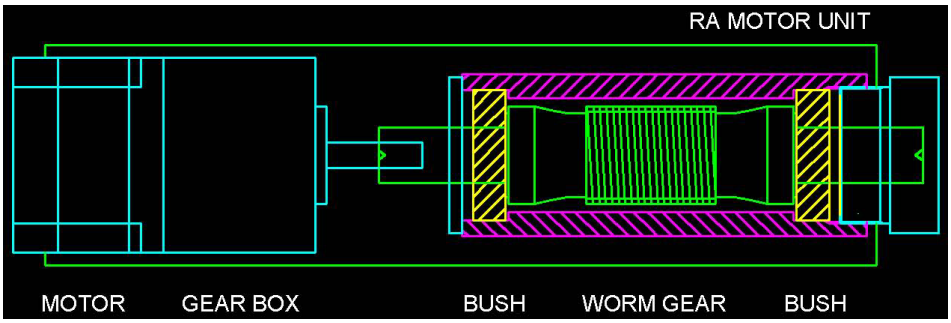

Figure 4. Sketch of the RA Motor unit.The RA Motor rotates the worm gear directly. This worm gear supported with two bushes, which are made by gunmetal.

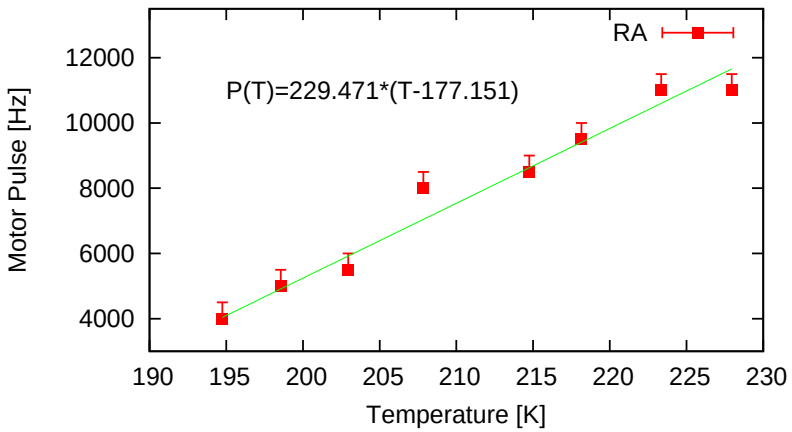

Figure 5. Result of the RA motor unit cold test. The horizontal axis is temperature [Kelvin] and the vertical axis is the motor pulse P [Hz]. We understood the major cause of motor rotation failure is the decrease of the space between the shaft and the bushes.

4. COLD TEST

AIRT40 will be used in not only summer but also in winter. AIRT40 has to work even at $-80°$C, so that we planned to test in a freezer. AIRT40 was too big to put it in the freezer as a whole, we disassembled it and tested four of the vital components individually: the RA motor unit, dec motor unit, focus unit, and RA shaft unit. These units include gears, shafts, bushes, and motors. These units are the most important packages to drive. If the units work individually even at $-80°$C, AIRT40 should work as a whole in low temperature.

4.1 RA Motor Unit

The RA and dec motors are 5-phase stepping motors (CSK564AP-T20, made by Oriental Motor Co., Ltd.). These motors are normal models. We exchanged the original grease for the Solvay Solexis FOMBLIN® ZLHT one. It is soft even at $-80°$C. Figure 4 is the sketch of the RA motor unit.

The worm gear which is made of steel is supported with two bushes, which are made of gunmetal (90% Cu and 10% Sn). Because the space between the worm gear shaft and the bushes decreases and the grease becomes thicker in low temperatures, the motor cannot rotate at high speed. When we treated the grease as a Newtonian fluid, the maximum motor pulse P (, which is in proportion to rotational velocity) becomes the following equation,

$$P(T) = C \times T^{\alpha}(T - T_C) \tag{1}$$

Where, T_C is the temperature when the space between the shaft and bushes becomes zero, α is a viscosity of the grease, and C is a proportional constant. Figure 5 shows the result of the RA motor unit cold test. The

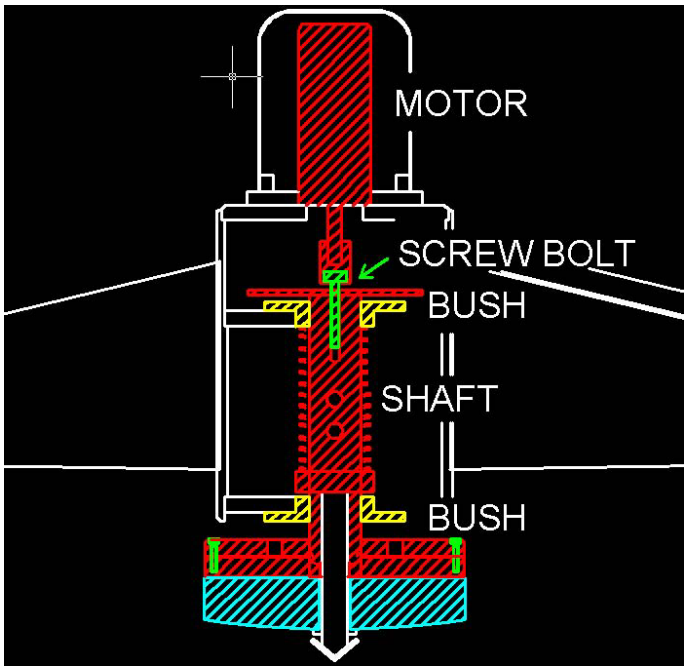

Figure 6. Sketch of the focus unit. For focusing, the motor rotates the screw bolt, thereby moving the secondary mirror up and down.

horizontal axis is temperature [Kelvin] and the vertical axis is the motor pulse P [Hz]. This result shows $\alpha \sim 0$ and that the maximum motor pulse is only in proportion to the temperature. In this result, we understood that the major cause of motor rotation failure is the decrease of the space between the shaft and the bushes. The outcome of the cold test of the dec motor was roughly the same as the RA one.

4.2 Focus Unit

The AIRT40 Focus Unit uses a 5-phase stepping motor CSK523AP-M30, which is made by Oriental Motor Co., Ltd. The secondary mirror was fixed to the shaft and supported by two bushes. This shaft and bushes are made from the same steel. For focusing, the motor rotates the screw bolt, thereby moving the secondary mirror up and down. Figure 6 show the sketch of the Focus Unit. We tested the Focus Unit in the freezer and verified that it could move even down to $-80°$C. This result means that the space between the shaft and the bushes hardly changes if these are made of the same material.

4.3 Worm Drive Unit

AIRT40 has two worm drives to reduce the rotational speed of the RA and dec motors. These worm drive units are made of various materials. For example, the RA/dec worms are made of brass, the shaft and bearings are made of steel, and the bearing holders are made of aluminum. Therefore, the backlash (the space between the worm screw and the worm wheel) changes depending on the temperature. The motor did not rotate at $-80°$C when the backlash was adjusted at 20°C. However once we adjusted the backlash at $-80°$C, the motor was able to move well.

5. TRACKING ERROR ANALYSIS

AIRT40 has an equatorial mount. An equatorial mount allows tracking an object by driving only the RA axis at a constant speed. However due to the set up error, the atmospheric refraction and a periodic error, it is not possible to track by driving only the RA axis. When we track an object whose position is (hour angle, declination)=(H, δ) for m minutes, this object moves $(\Delta\alpha_m, \Delta\delta_m)$ in the telescope field of view. (The unit is the arcsecond.)

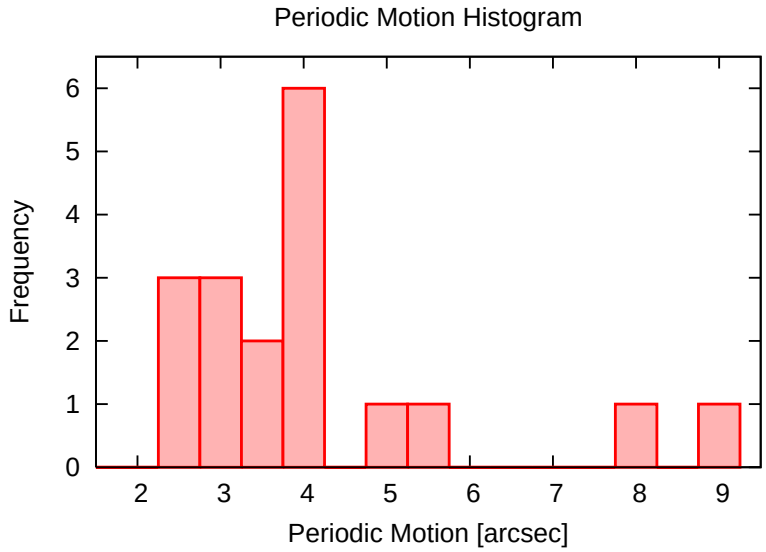

Figure 7. Histogram of the amplitude of the periodic motion error observed at Sendai. The average of periodic motion P_0 is 4.3 ± 1.8 [arcsecond]. This accuracy is not generally good, although it is enough for the 2010-2011 summer campaign at Dome Fuji.

$$\begin{aligned}\Delta\alpha_m &= \left\{ 902''.465 \times \left(\frac{\cos\delta \sin H_0}{\cos\delta \sin H_0 - 4.84814 \times 10^{-6} \epsilon_p'' \sin H_p \sin\delta} - 1 \right) \right. \\ &\quad \left. -0''.255078 \times \frac{\sin\delta \sin L \cos L \cos H_0 + \cos\delta \cos^2 L}{(\sin\delta \sin L + \cos\delta \cos L \cos H_0)^2} \right\} m \\ &\quad + P_0'' \{\sin(1.57510m + \phi) - \sin\phi\} \qquad (2) \\ \Delta\delta_m &= \left\{ -4.37527 \times 10^{-3} \epsilon_p'' \sin(H_0 - Hp) + 0''.255078 \times \frac{\sin L \cos L \sin H_0}{(\sin\delta \sin L + \cos\delta \cos L \cos H_0)^2} \right\} m \qquad (3)\end{aligned}$$

Here, H_0 and ϵ_p mean the hour angle and the separation angle of the set up error respectively, and L is the latitude of the observatory. P_0 and ϕ show the periodic motion amplitude and phase, respectively. Figure 7 shows the histogram of the amplitude of the periodic motion error observed at Sendai, Japan. This histogram shows that the periodic motion P_0 is about 4.3 ± 1.8 [arcsecond]. This accuracy is not generally good, although it is enough for the 2010-2011 summer campaign at Dome Fuji. Because of no sunset during summer, the sky background is too high to use long exposure times.

6. POINTING ERROR ANALYSIS

In general, a telescope has three axes (RA, dec, and opt axis). These three axes should be orthogonal, althought the telescope as built is not quite orthogonal. Because of this, telescope has pointing error. In addition, the errors of the setup, the atmospheric refraction, a periodic motion, and a backlash also exist. When AIRT40 is aligned using the object A (hour angle, declination)=(H_A, δ_A) and then points to the object B (H_B, δ_B), the pointing errors of the RA and dec axis ($\Delta\alpha_p$, $\Delta\delta_p$)are given below,

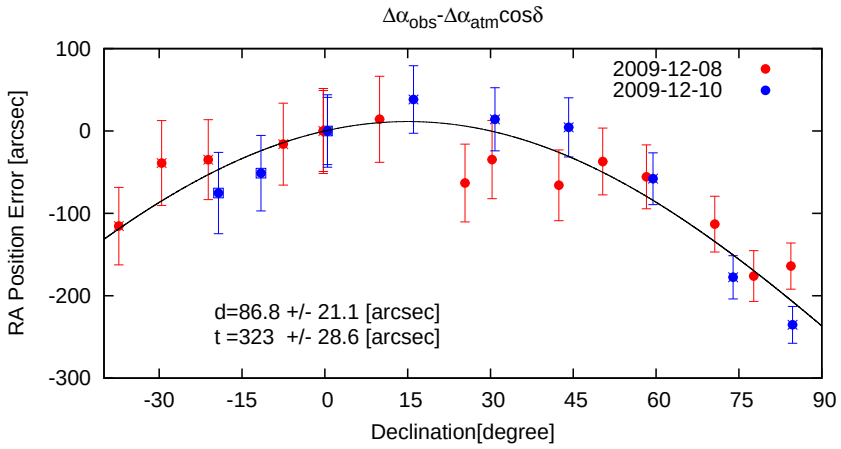

Figure 8. RA pointing errors observed at various stars. The horizontal axis is the declination angle [degree] of the stars used for this observation and the vertical axis is the RA pointing errors [arcsecond]. The error bars are evaluated from the periodic motion P_0 and the resolution of the AIRT40 control software.

$$\begin{aligned}
\Delta\alpha_p \simeq & \left[\epsilon''_p\Big\{\sin(H_B-H_p)\tan\delta_B-\sin(H_A-H_p)\tan\delta_A\Big\}\right. \\
& \left.+d''\Big(\tan\delta_B-\tan\delta_A\Big)-t''\left(\frac{1}{\cos\delta_B}-\frac{1}{\cos\delta_A}\right)\right]\cos\delta_B\pm|P''_0|\Big(\cos\delta_A+\cos\delta_B\Big) \\
& -58''.3\times\left(\frac{\sin H_B\cos L}{\sin\delta_B\sin L+\cos\delta_B\cos L\cos H_B}-\frac{\sin H_A\cos L}{\sin\delta_A\sin L+\cos\delta_A\cos L\cos H_A}\right) \qquad (4) \\
\Delta\delta_p \simeq & \; 58''.3\times\left\{\frac{\sin L}{\sin\delta_B\cos\delta_B\sin L+\cos^2\delta_B\cos L\cos H_B}\right. \\
& \left.-\frac{\sin L}{\sin\delta_A\cos\delta_A\sin L+\cos^2\delta_A\cos L\cos H_A}-\Big(\tan\delta_B-\tan\delta_A\Big)\right\} \\
& +\epsilon''_p\Big\{\cos(H_B-H_p)-\cos(H_A-H_p)\Big\}\pm 2|B''| \qquad (5)
\end{aligned}$$

Here, d means the orthogonal error between the RA axis and the dec axis. The orthogonal error between the dec axis and the opt axis is t. B means the dec backlash. All units are in arcseconds. Figure 8 shows the RA pointing errors observed at various stars. The horizontal axis is the declination angle [degree] of the stars used for this observation and the vertical axis is the RA pointing errors [arcsecond]. The error bars are evaluated from the periodic motion P_0 and the resolution of the AIRT40 control software. From this observation, we find that there are orthogonalization errors $d = 87 \pm 21$ [arcsecond] and $t = 320 \pm 29$ [arcsecond] in AIRT40. The inclination d between the RA axis and the dec axis can be adjusted using shims. However it is impossible to adjust the angle t between the dec axis and the opt axis, because the opt axis should be adjusted for optical alignment. We plan to use AIRT40 with Mode-A TONIC2 in the 2010-2011 summer campaign. The field of view of Mode-A is only $\phi 5$ [arcminute]. This means that it is impossible to point to an object automatically. However there are observers in the Dome Fuji during this campaign, so that it is easy to correct the pointing error manually. In the winter-over observation during 2012-2014, we will use AIRT40 with Mode-B TONIC2, which has wide field of view ($\phi 30$ [arcminute]). This needs no manual correction because the Mode-B field of view is far larger than the total pointing error. Therefore, AIRT40 should be able to point the object without trouble.

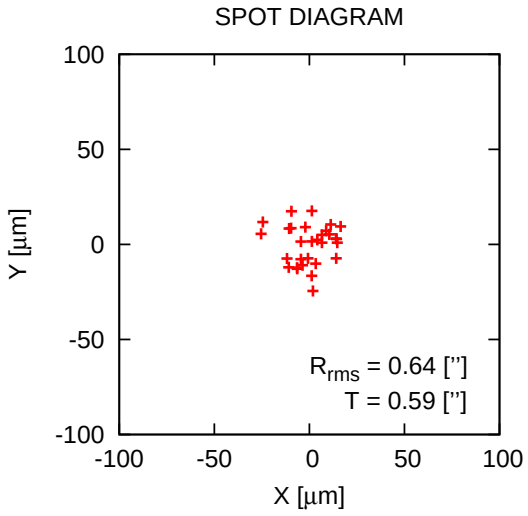

Figure 9. Spot diagram obtained with Hartmann test. The horizontal axis and vertical axis are true scale on the focal plane [μm]. As a result of this observation, AIRT40's Hartmann constant T was 0.59 [arcsecond].

7. OPTICAL ANALYSIS

AIRT40 is a Classic Cassegrain telescope which has a parabolic primary mirror and a hyperbolic secondary mirror. This optical system has no spherical aberration. However this is an ideal. In fact, the performance of AIRT40 decreases because there are some tolerances and miss alignments. Besides, the optical axis of AIRT40 shifts easily during transportation. Furthermore, no man can align the optics perfectly. The most important thing is to achieve the accuracy which is needed for observations. Therefore, we carried out the Hartmann test to check the potential of AIRT40's optics and the accuracy of the optical alignment.

7.1 Hartmann test

The Hartmann test is a way of checking the accuracy of the shape of the mirrors and the alignment of the telescope.[7] This test uses a "Hartmann plate," which has a number of small holes installed on the top ring of AIRT40. If the optical system of AIRT40 is perfect, starlight passes these small holes and converges at the focal plane. Although the aberrations, tolerances and/or miss alignments cause the light to diverge. Then, the imaging ability at the focal plane is evaluated by taking images with the focus shifted forwards and backwards with respect to the ideal focal plane. Figure 9 shows the spot diagram obtained with Hartmann test. The horizontal axis and vertical axis are true scale on the focal plane [μm]. As a result of this observation, AIRT40's Hartmann constant T was 0.59 [arcsecond]. This result is worse than the result of last time ($T = 0.33$ [arcsecond]).[6] From the analysis of the tolerance of this optical system, it is thought that this difference is caused by the miss alignment of the optical system. AIRT40 is the telescope for infra-red observation; the diffraction limit of K-band is 1.4 [arcsecond]. This Hartmann constant $T = 0.59$ [arcsecond] is no problem for the infra-red imaging.

8. OBSERVATION PLAN

We will perform site-testing and astronomical observation at Dome Fuji during the austral summer of 2010-2011. This is the first observation to use an optical/infra-red telescope at Dome Fuji. We propose the observation plans to use AIRT40 as follows.

8.1 Seeing measurement

Seeing is a parameter that describes how blurry a star image will be. It is caused by atmospheric turbulence and is the apparent angular diameter of a point source measured in arcsecond. The DIMM (Differential Image Motion Monitor) which is now broadly used for site testing over the world is a technique to measure seeing

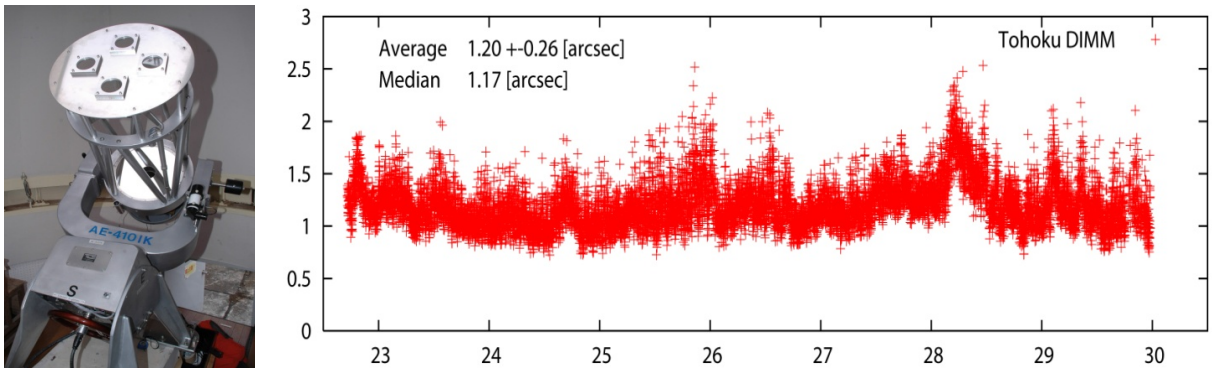

Figure 10. Left: A picture of the Tohoku DIMM on the top ring of AIRT40. Right: A result of the test observation at Sendai, Japan. The horizontal axis is local time (For example, 25 means 1 am, 26 means 2 am, etc.) and the vertical axis means the apparent angular diameter; seeing. The unit is the arcsecond.

using a small telescope. We developed the Tohoku DIMM, referred to as UT-DIMM[5] optimized for summer-time observation at Dome Fuji. To measure the seeing even in daytime, we made the aperture as large as possible and added the baffle to get high contrast images. We plan to measure the seeing using Canopus (α Carinae, -0.72 mag.), which is one of the brightest star in this campaign.

Figure 10 shows a picture of the Tohoku DIMM and a result of test observation at Sendai, Japan. We measured the seeing using Capella (α Aurigae, 0.1 mag.) at this time. The horizontal axis is local time (For example, 25 means 1 am, 26 means 2 am, etc.) and the vertical axis means the apparent angular diameter; seeing [arcsecond]. Here, the sunrise of this day was about 29:30. It is shown by this test observation that limited seeing measurements in daytime are possible. From this result, it can also be said that the seeing measurement at Dome Fuji is very possible. We will measure the value and time variation of the seeing for 3-days of continuous observation.

8.2 Measurement of the daytime infra-red sky background

The Sky background is one of the important parameters to decide the limiting magnitude.[3] The day-time sky background is caused by the Rayleight scattering and Mie scattering of the sun by the atmosphere. Here, we expect that the strength of the scattering is much lower because there is no air pollution in the Antarctic plateau. Moreover, the scattering depends on wavelength; the infra-red scattering is weaker than visible. Therefore, we examine if infra-red astronomical observation is possible even in daytime by measuring the daytime infra-red sky background. We will measure the infra-red sky background by observing the sky at various positions using AIRT40 with Mode-A TONIC2.

8.3 Continuous observation of Venus

We plan to perform the continuous observations of Venus. Venus rotates once every 243 Earth days, though the atmosphere at the cloud tops rotates in just four Earth days. This is called "super-rotation". This mechanism is still not understood in detail. It is possible to observe Venus continuously because like the sun, it doesn't set during summer in Antarctica. In this observation we will use AIRT40 with Mode-A TONIC2, it can take Venus images with high signal to noise ratio even in daytime. Then, we plan to observe Venus continuously for a week at infra-red wavelengths and examine the cloud structure by following the movement of the cloud of Venus.

9. CONCLUSION

Dome Fuji, on the Antarctic plateau, is expected the best site for infra-red astronomy on Earth. To enjoy these advantages, we are planning to construct 2m-class infra-red telescopes at Dome Fuji. For this purpose we developed the Antarctic Infra-Red Telescope with a 40cm primary mirror (AIRT40), which will be the first optical/infra-red telescope setting up at Dome Fuji. We repeated the freezer cold tests, and confirmed that

AIRT40 can work well even at $-80°$C. We also confirmed that this telescope has enough pointing, tracking, and optical accuracy for the 2010-2011 observation by the test observations at Sendai, Japan. Therefore, we think that AIRT40 is suited to observe at Dome Fuji. We plan to observe the seeing, infra-red sky background, and Venus using AIRT40 during the 2010-2011 austral summer campaign.

ACKNOWLEDGMENTS

This work has been supported by a Grant-in-Aid for Scientific Research (21244012) of the Ministry of Education, Culture, Sports, Science, and Technology in Japan, and be supported by a grant from the Hayakawa Satio Fund awarded by the Astronomical Society of Japan.

REFERENCES

[1] Agabi, A., Aristidi, E., Azouit, M., Fossat, E., Martin, F., Sadibekova, T., Vernin, J. and Ziad, A., "First Whole Atmosphere Nighttime Seeing Measurements at Dome C, Antarctica," *Publications of the Astronomical Society of the Pacific* **118**, 344-348 (2006)

[2] Ishii, S., Seta, M., Nakai, N., Nagai, S., Miyagawa, N., Yamauchi, A., Motoyama, H. and Taguchi, M., "Site testing at Dome Fuji for submillimeter and terahertz astronomy: 220 GHz atmospheric-transparency," *Polar Science* **3**, 213-221 (2010)

[3] Krisciunas, K. and Schaefer, B. E., "A model of the brightness of moonlight," *Publications of the Astronomical Society of the Pacific* **103**, 1033-1039 (1991)

[4] Lawrence, J. S., Ashley, M. C. B.; Tokovinin, A. and Travouillon, T., "Exceptional astronomical seeing conditions above Dome C in Antarctica," *Nature* **431**, 278-281 (2004)

[5] Motohara, K., Doi, M., Soyano, T., Tanaka, M., Kohno, K., Miyata, T., Takato, N. and Uraguchi, F., "University of Tokyo DIMM: a portable DIMM for site testing at Atacama," *Proc. SPIE* **5382**, 648-655 (2004)

[6] Murata, C., Ichikawa, T., Lundock, R. G., Taniguchi, Y. and Okita, H., "A 40cm Infra-Red Telescope in Antarctica," *Proc. SPIE* **7012**, 291-298 (2008)

[7] Pyo, T., Tanaka, M., Nakamura, K. and Tanaka, W., "Estimation of the optical property and the pointing accuracy of the infra-red simulator," *Report of the National Astronomical Observatory of Japan* **3**, 99-115 (1998)

[8] Saunders, W., Lawrence, J. S., Storey, J. W. V., Ashley, M. C. B., Kato, S., Minnis, P., Winker, D. M., Liu, G. and Kulesa, C., "Where Is the Best Site on Earth? Domes A, B, C, and F, and Ridges A and B," *Publications of the Astronomical Society of the Pacific* **121**, 976-992 (2009)

[9] Takato, N., Uraguchi, F., Motoyama, H., Fukui, K., Tanuchi, M., Ichikawa, T., Taniguchi, Y. and Murata, C., "Preliminary evaluation of Dome Fuji as a possible site for an infra-red astronomical observatory -SODAR measurement of atmospheric turbulence in the boundary layer in Antarctic summer-," *Antarctic Record* **52**, 182-192 (2008)

[10] Yamanouchi, T., Hirasawa, N., Hayashi, M., Takahashi, S. and Kaneto, S., "Meteorological characteristics of Antarctic Inland Station, Dome Fuji," *Memoirs of National Institute of Polar Research* **57**, 94-104 (2003)

[11] Yang, H., Allen, G., Ashley, M.C.B., Bonner, C.S., Bradley, S., Cui, X., Everett, J.R., Feng, L., Gong, X., Hengst, S., Hu, J., Jiang, Z., Kulesa, C.A., Lawrence, J.S., Li, Y., Luong-Van, D., McCaughrean, M.J., Moore, A.M., Pennypacker, C., Qin, W., Riddle, R., Shang, Z., Storey, J.W.V., Sun, B., Suntzeff, N., Tothill, N.F.H., Travouillon, T., Walker, C.K., Wang, L., Yan, J., Yang, J., York, D., Yuan, X., Zhang, X., Zhang, Z., Zhou, X. and Zhu, Z., "The PLATO Dome A Site-Testing Observatory: Instrumentation and First Results," *Publications of the Astronomical Society of the Pacific* **121**, 174-184 (2009)

[12] Yang, H., Kulesa, C. A., Walker, C. K., Tothill, N. F. H., Yang, J., Ashley, M. C. B., Cue, X., Feng, L., Lawrence, J. S., Luong-Van, D. M., Storey, J. W. V., Wang, L., Zhou, X. and Zhu, Z., "Exceptional terahertz transparency and stability above Dome A, Antarctica," *Publications of the Astronomical Society of the Pacific* **122**, 490-494 (2010)